Colloids and Surfaces B: Biointerfaces 89 (2012) 79–85

Contents lists available at SciVerse ScienceDirect

Colloids and Surfaces B: Biointerfaces

journal homepage: www.elsevier.com/locate/colsurfb

Synthesis, dispersion, and cytocompatibility of graphene oxide and reduced graphene oxide

Malgorzata Wojtoniszak[a,*], Xuecheng Chen[a], Ryszard J. Kalenczuk[a], Anna Wajda[b], Joanna Łapczuk[b], Mateusz Kurzewski[b], Marek Drozdzik[b], Pual K. Chu[c], Ewa Borowiak-Palen[a]

[a] Westpomeranian University of Technology in Szczecin, Department of Environmental and Chemical Engineering, Pulaskiego 10, 70-322 Szczecin, Poland
[b] Pomeranian Medical University, Department of Pharmacokinetics and Therapeutic Drug Monitoring, Powstańców Wlkp. 72 Av., 70-111 Szczecin, Poland
[c] Department of Physics and Materials Science, City University of Hong Kong, Tat Chee Avenue, Kowloon, Hong Kong, China

ARTICLE INFO

Article history:
Received 30 June 2011
Received in revised form 30 August 2011
Accepted 30 August 2011
Available online 7 September 2011

Keywords:
Graphene oxide
Graphene
In vitro toxicology

ABSTRACT

The synthesis, characterization, and toxicity of graphene oxide and reduced graphene oxide are reported. Prior to the cytocompatibility tests the stability of the suspensions in a wide range of concentrations (3.125-100 μg/mL) of three different dispersants is studied. Polyethylene glycol (PEG), polyethylene glycol–polypropylene glycol–polyethylene glycol (Pluronic P123), and sodium deoxycholate (DOC) are investigated as the dispersants. The toxicity depends on the type of dispersant and concentration of the nanomaterials in the suspensions. Detailed analysis suggests that graphene oxide functionalized with PEG in the concentration range between 3125 μg/mL and 25 μg/mL exhibits the best biocompatibility with mice fibroblast cells (line L929).

© 2011 Elsevier B.V. All rights reserved.

1. Introduction

Recently, graphene and its derivatives have been investigated extensively. This is due its exceptional mechanical, electrical, thermal and optical properties, high surface area-to-volume ratio, and unique atomic structure. Therefore, many applications are expected, for instance, electronic devices, composites and nanomedicine [1–5]. Although carbon nanotubes have been widely investigated in the biomedical field such as drug delivery, biosensing, and molecular imaging [6–8], biomedical properties like pharmacokinetics, toxicity, and cytocompatibility of graphene and graphene oxide have not been systematically explored. Yang et al. [9] have reported pharmacokinetics and biodistribution of graphene functionalized with PEG (polyethylene glycol) and examined the toxicity in mice. Their results reveal that graphene/PEG does not induce appreciable toxicity at an administered dose of 20 mg/kg for 3 months. PEGylated graphene oxide in a physiological solution has been employed in cell imaging and drug delivery [10,11]. Wang et al. [12] have suggested dose- and time-dependent cytotoxicity of graphene oxide, which can enter the cytoplasm and nucleus, decrease cell adhesion, and induce apoptosis. In spite of previous studies, the systematic investigation on the preparation and monitoring of the stability of graphene or graphene oxide suspensions in different dispersants are still required. Therefore, in this paper we report the synthesis of graphene oxide and reduced graphene oxide as well as stable suspension formation in different dispersants. The concentration effects on mice fibroblast cells (L929) are also investigated. As a result of this study the most biocompatible system based on graphene derivative is proposed.

2. Materials and methods

Graphene oxide (GO) was synthesized by oxidation of natural graphite flakes (Aesar, 325 mesh) according to the modified Hummers method [13]. Concentrated sulfuric acid and orthophosphoric acid (120:15 mL) were added to a mixture of $KMnO_4$ (6 g) and graphite (1 g). It was heated to 50 °C and stirred for 24 h. The resulting mixture was poured into ice (150 mL) and H_2O_2 (30%, 1 mL) and then filtered using a polycarbonate membrane. The solid product was washed with water, 30% HCl, and ethanol two times before vacuum drying for 12 h.

Before the reduced graphene oxide was synthesized, the GO was exfoliated in water by ultrasonication to produce a homogeneous graphene oxide water based suspension (0.1 mg/mL). The GO was then reduced using glucose as the reducing agent at 95 °C for 2 h [14]. Afterwards, the mixture was filtered by a polycarbonate membrane and washed several times with water and ethanol to obtain reduced graphene oxide (RGO).

Before the cytocompatibility tests, the stability of the dispersions in phosphate buffered saline (PBS) containing three types of

* Corresponding author. Tel.: +48 914494772.
E-mail address: m.wojtoniszak@zut.edu.pl (M. Wojtoniszak).

0927-7765/$ – see front matter © 2011 Elsevier B.V. All rights reserved.
doi:10.1016/j.colsurfb.2011.08.026

dispersants, PEG, DOC and Pluronic P123, was studied. Aqueous solutions of PEG, DOC and Pluronic P123 (1 mg/mL) were prepared. Afterwards, GO and RGO were added to the solutions (1 mg/mL). Next, the GO and RGO suspensions were diluted with PBS and sonicated to reach the following concentrations: 100 μg/mL, 50 μg/mL, 25 μg/mL, 12.5 μg/mL, 6.25 μg/mL, and 3.125 μg/mL. The concentration of the surfactants in the suspensions was also adjusted to 100 μg/mL, 50 μg/mL, 25 μg/mL, 12.5 μg/mL, 6.25 μg/mL, and 3.125 μg/mL. In order to assess the suspensions homogeneity, the UV/vis intensity at 325 nm was plotted against the sonication time. Finally, the stability of the homogeneous dispersions was examined by monitoring the change of UV/vis absorbance (at 325 nm) after 4 h, 24 h and 48 h.

The cytocompatibility of the graphene oxide and reduced graphene oxide biofunctionalized with PEG, DOC or Pluronic P123 was assessed using the WST-1 test (Roche Applied Science, Mannheim, Germany). The cell proliferation WST-1 test is based on the reduction of the tetrazolium salt WST-1 to a soluble red-colored formazan by mitochondrial dehydrogenase of metabolically active cells. The amount of formazan dye is directly correlated to the number of metabolically active cells. In our experiments, the mouse fibroblast cells (L929) were seeded into a 96-well plate at a density of 7.4×10^3/well and then cultured in a humidified incubator with 5% CO_2 at 37 °C. The cell culture medium (DMEM, Sigma–Aldrich) was supplemented with 10% of fetal bovine serum (FBS, Gibco) and 0.4% streptomycin/penicillin. After an incubation period of 24 h, the L929 cells were treated with graphene oxide and reduced graphene oxide suspensions of PEG, DOC, Pluronic P123 with different concentrations (0 (only medium with added dispersant – reference suspension), 3.125, 6.25, 12.5, 25.0, 50.0, and 100.0 μg/mL) for 48 h. In this way the toxicity dependence on the type of dispersant and nanomaterials concentration were investigated. After this incubation period, WST-1 reagent was added for 30 min and the absorbance was measured on a microplate spectrophotometer at 450 nm. The blank absorbance (medium without cells) was subtracted from each value. All the experiments were conducted in triplicate.

High-resolution transmission electron microscopy (HR-TEM) (FEI Tecnai F30) was employed to examine the morphology of the graphene oxide and reduced form. Thermogravimetric analysis was performed on the SDT Q600 Simultaneous TGA/DSC under an air flow of 100 mL min^{-1} and at a heating rate of 5 °C min^{-1}. Raman spectra were acquired on the inVia Raman Microscope (Renishaw) at an excitation wavelength of 514 nm. Before the analysis, the samples were deposited on a SiO_2/Si wafer (300 nm SiO_2). The UV/vis absorption spectra were recorded using a Helios Gamma UV–vis spectrometer and IR absorption spectra were acquired on the Nicolet 6700 FT-IR spectrometer. XRD was performed using the X'Pert Philips Diffractometer with a Cu anode ($K_{\alpha 1}$ = 1.54056 Å) to determine the structure.

3. Results

To investigate the oxidation and reduction processes, IR spectra were obtained from the starting graphite, graphene oxide, and reduced graphene oxide. Fig. 1A depicts the IR spectrum of the starting graphite and only peaks attributable to C=C (graphitic carbon atoms vibrations) and C–O (CO_2 in environment) are detected. Fig. 1B shows the IR spectrum of the GO and the following absorption modes are detected: 1620 nm due to the aromatic C=C bond, 1060 nm attributed to the C–O stretching vibration mode in the alkoxy group, at 1170 nm assigned to the epoxy C–O stretching peak, at 1400 nm arising from the C–OH carboxyl group, at 1740 nm corresponding to the C=O stretch mode in the carboxyl group, 2930 nm originating from C–H, and 3420 nm from O–H groups

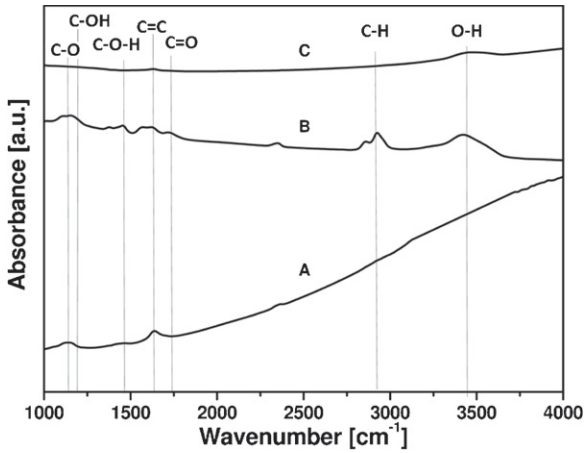

Fig. 1. IR spectra of graphite (A), graphene oxide (B) and reduced graphene oxide (C).

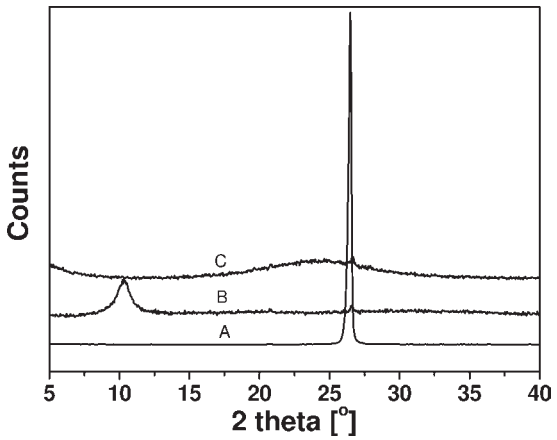

Fig. 2. XRD patterns of graphite (A), graphene oxide (B) and reduced graphene oxide (C).

[15–17]. The results indicate that the graphite is successfully oxidized and probably cleaved in the form of GO. In the next step, the GO is reduced by glucose and as shown in Fig. 1C, the IR spectrum of the RGO indicates significant reduction of the intensity of all oxygen containing moieties suggesting efficient conversion of graphene oxide to reduced graphene oxide.

XRD is a useful tool to assess the efficiency of the process by monitoring the crystal structure. Fig. 2 shows the XRD patterns of graphite (A), graphene oxide (B), and reduced graphene oxide (C). Each pattern in the reported 2θ range is dominated by peaks at 26.475°, 10.375°, and 24.625° in graphite, GO, and RGO, respectively. The interlayer distance of GO is approximately 8.5 Å which is enhanced to that of graphite (3.4 Å, 2θ = 26.475°). This phenomenon can be attributed to the introduction of oxygen-containing functional groups into the carbon lattice during the oxidation. After reduction, the peak at 10.375° vanishes and a new peak at 24.625° appears. This can be ascribed to the removal of functional groups and may indicate complete deoxygenation of graphene oxide and exfoliation of graphene [18].

Fig. 3 presents the TGA curves of graphite, graphene oxide, and reduced graphene oxide based on the mass loss during the heating in air. Graphene oxide shows mass losses at two temperature ranges (Fig. 3B). The first one, between 120 °C and 300 °C, corresponds to the removal of oxygen-containing functional groups [19]. Whereas the second one occurs, at approximately 500 °C, due to the bulk pyrolysis of the carbon skeleton [20]. It is also observed in graphite at 700 °C (Fig. 3A) and in RGO at 400 °C (Fig. 3C).

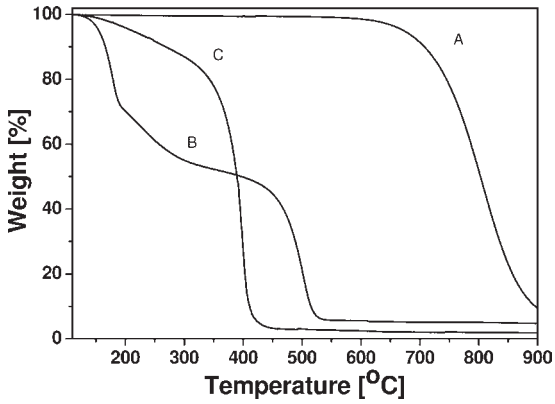

Fig. 3. TGA curves of graphite (A), graphene oxide (B) and reduced graphene oxide (C).

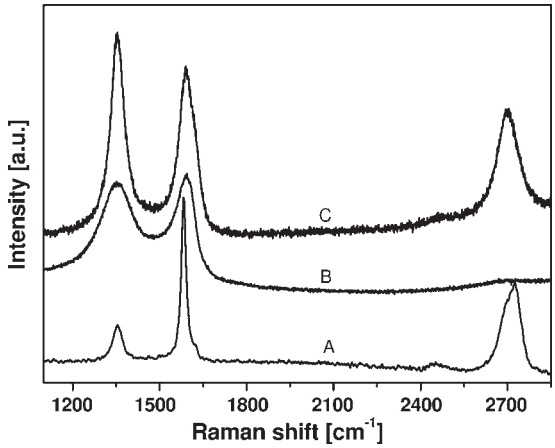

Fig. 4. Raman spectra of graphite (A), graphene oxide (B) and RGO (C).

The TGA analysis indicates incomplete reduction of the functional groups because roughly 13 wt% of oxygen containing groups did not undergo reduction. It means that reduction time could be extended.

Raman spectroscopy is usually used to determine the graphene structure and to identify the number of layers. Here, micro-Raman measurements are performed meaning that the individual flakes are analyzed and the typical spectra are presented in Fig. 4. Each spectrum shows three main peaks. The G band at approximately 1580 cm^{-1} originates from the in-plane vibration of sp^2 carbon atoms and is a doubly degenerate phonon mode (E_{2g} symmetry) at the Brillouin zone center [21]. The 2D band (at roughly 2700 cm^{-1}) originates from a two phonon double resonance Raman process [22], and the D peak around 1355 cm^{-1} is a breathing mode of A_{1g} symmetry involving phonons near the K zone boundary [23]. As shown in the Raman spectrum of graphene oxide (Fig. 4B), the G band broadens and up-shifts in comparison to those observed in graphite (from 1581 cm^{-1}, Fig. 4A to 1591 cm^{-1}). A possible explanation of this behaviour is the presence of isolated double bonds which resonate at higher frequencies [24]. In the reduced graphene oxide (Fig. 4C) the G band down-shifts to the position close to the G band of graphite [1586 cm^{-1}] and this is attributed to graphitic "self-healing" [24]. Furthermore, the D band at 1355 cm^{-1} becomes prominent, indicating that the oxidation process influences the size of the in-plane sp^2 domains [23]. The 2D peak observed from RGO also shows significant change in the shape compared to graphite. It has been proposed by Ferrari et al. [25] that the number of layers in few-layered graphene may be distinguished by the shape, width, and position of the 2D peak. In the 2D peak of RGO, the position at 2698 cm^{-1} and its shape suggest 3- or 4-layered graphene. The data indicate that the obtained RGO is composed of few-layered graphene (FLG).

To further characterize the structure of graphene oxide and reduced graphene oxide, transmission electron microscopy is used. Fig. 5 shows the TEM images of the materials indicating that the graphene oxide (A and B) as well as reduced graphene oxide (C and D) has the tendency to scroll and wrinkle. The length of the reduced graphene oxide and graphene oxide is observed to be between 100 and 350 nm.

Because of its low toxicity, PEG is a promising compound in biomedical applications associated with biofunctionalized graphene oxide and graphene [26]. Researchers have recently suggested dose- and time-dependent toxicity of PEGylated graphene oxide [10]. This phenomenon may be explained by investigation of the stability of the suspensions. As shown in Fig. 6, the UV–vis absorbance (at 325 nm) is presented as a measure of the homogenization process of the GO and RGO dispersions in PBS and PEG, DOC, or Pluronic P123 (at a concentration of 100 μg/mL). The homogenized solution is diluted to the desired concentration and the stability of the suspension is illustrated in Fig. 7. The UV–vis absorbance variation at 325 nm observed from the graphene oxide and reduced graphene oxide suspensions versus the time is presented. In each case, the absorbance of the suspensions with the concentration of the materials between 100 μg/mL and 50 μg/mL diminishes significantly after 48 h. At lower concentrations, the graphene oxide as well as reduced graphene oxide exhibits higher stability. It should be noted that the absorbance of the graphene oxide dispersion starts to increase after 4 h when the materials are dispersed in PEG (Fig. 7A, concentration 12.5 μg/mL, 6.25 μg/mL, 3.125 μg/mL), DOC (Fig. 7B, concentration 6.25 μg/mL, 3.125 μg/mL), Pluronic P123 (Fig. 7C, concentration 25 μg/mL, 3.125 μg/mL). This may be attributed to the agglomeration of the particles previously suspended in solution.

The cytocompatibility results in Fig. 8 indicate that the dispersant used to stabilize the suspension, type of materials, and its concentration significantly influence the cell toxicity. As shown, graphene oxide and reduced graphene oxide in the three different dispersants, the graphene oxide functionalized with PEG exhibits the lowest toxicity. The viability of L929 cells decreases to 36.3% (vs. free growing cells) when they are exposed to graphene oxide functionalized with PEG at a concentration of 100 μg/mL. With regard to the GO functionalized with other dispersants, the viability decreases to 15.5% and 6.3%, for DOC and Pluronic P123, respectively. Our study on reduced graphene oxide discloses better cytocompatibility of RGO biofunctionalized with PEG in respect to DOC and Pluronic P123. The cells exposed to the suspension of RGO/PEG at concentrations between 3.125 μg/mL and 25 μg/mL show relatively high viability (from approximately 95% to over 60% vs. free growing cells with reference suspension). When the concentration exceeds 25 μg/mL, the viability diminishes suddenly. Similar results are observed for RGO functionalized with DOC. The reduced graphene oxide functionalized with Pluronic P123 appears to be the most toxic.

4. Discussion

The cytocompatibility of the functionalized graphene oxide and reduced graphene oxide is analyzed along with the potential biological effects of the used dispersants in L929 mouse fibroblasts. L929 mouse fibroblasts are the most commonly used standardized established cell line for assessing cytotoxicity in biomaterial evaluation. International Standards Organization (ISO) has recommended preliminary cytotoxic screening (ISO 7405 Part 5) with these cells [27]. The highest cytocompatibility is observed for PEG

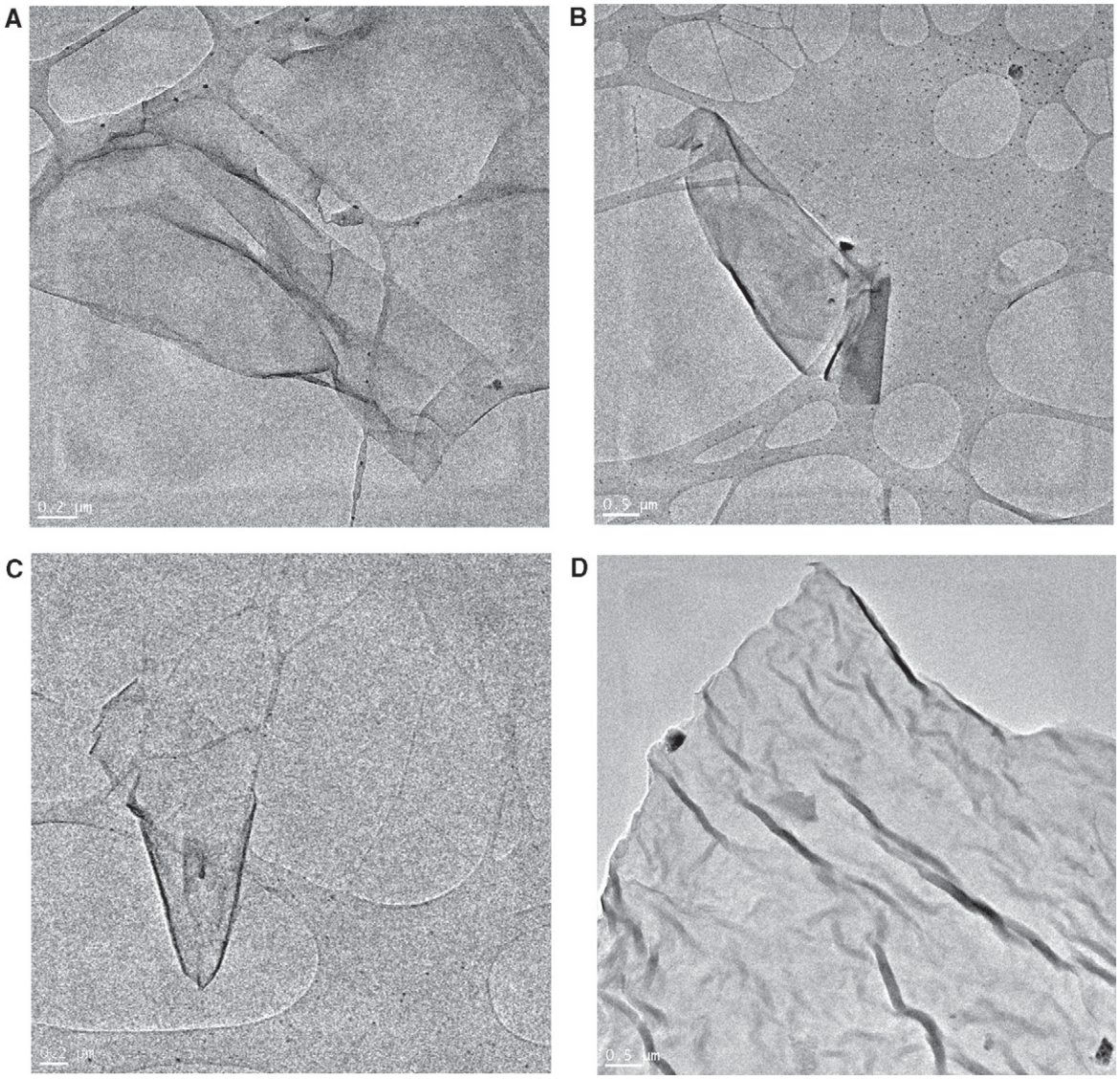

Fig. 5. TEM images of graphene oxide (A) and reduced graphene oxide (B).

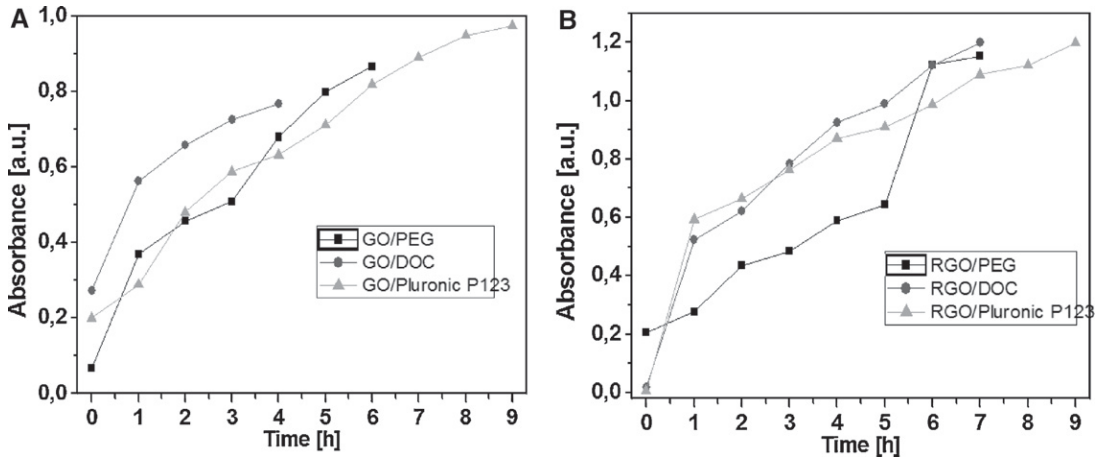

Fig. 6. UV/vis absorbance at 325 nm as a measure of homogenization process of the dispersions of graphene oxide and reduced graphene oxide in PEG, DOC and Plruronic P123 with concentration of 100 μg/mL.

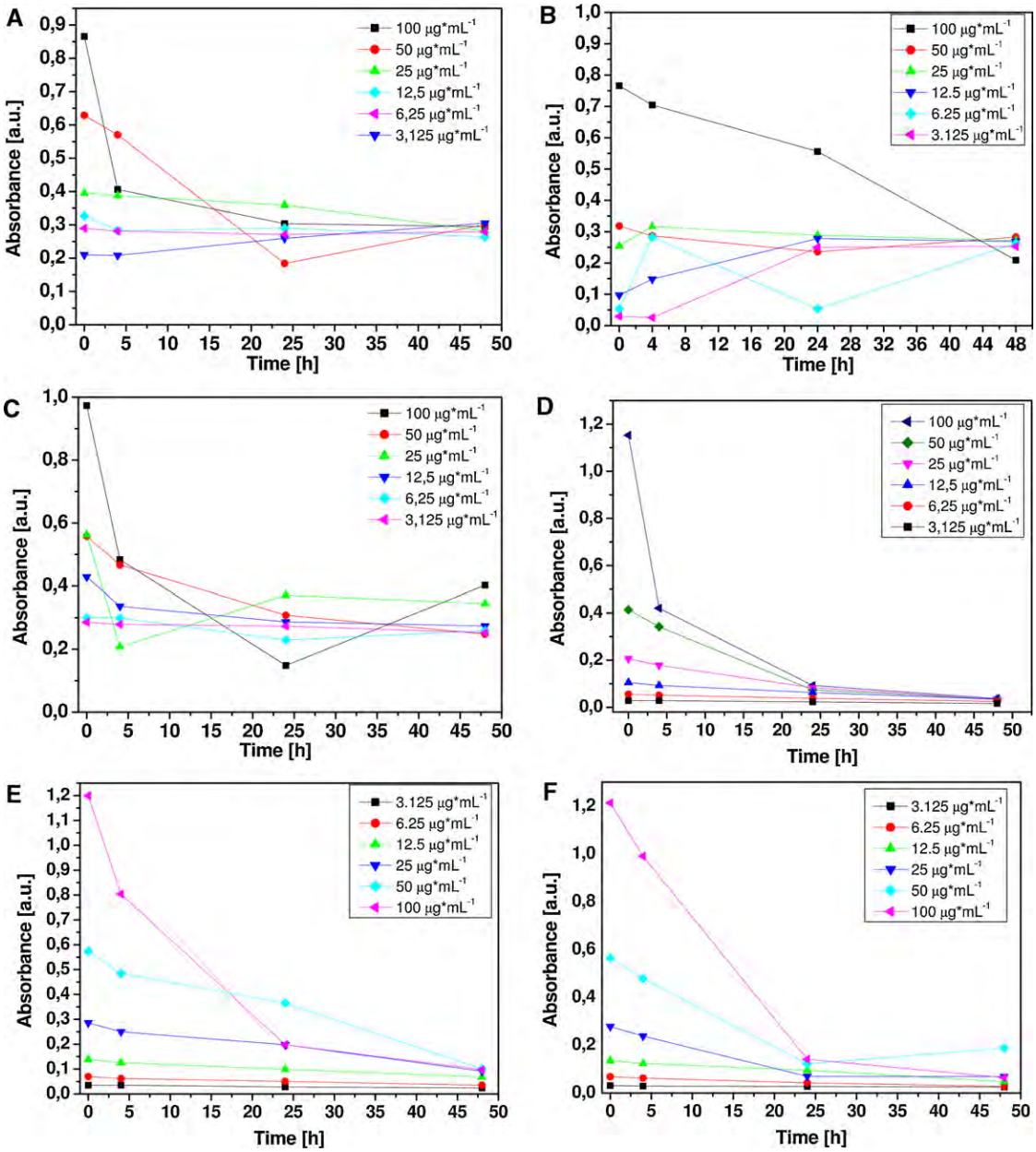

Fig. 7. UV–vis absorbance at 325 nm variation as a measure of stability of the dispersions of graphene oxide in PEG (A), DOC (B), Pluronic P123 (C) and reduced graphene oxide in PEG (D), DOC (E), Pluronic P123 (F).

and potential toxicity for DOC and Pluronic P123. Therefore, the reduced L929 cell viability in the case of the functionalized GO and RGO depends on the dispersants. Feng et al. [28] reported that at high concentrations (up to 300 μg/mL), polyethyleneimine (PEI) graphene complexes showed slightly higher relative HeLa (human epithelial carcinoma) cell viability compared to graphene oxide, possibly due to the improved stability of GO-PEI in the physiological environment. Similar dose-dependent toxic effects of graphene oxide were reported by Chang et al. [29] and Zhang et al. [30]. The studies were carried out using the A549 cells [29], human lung carcinoma epithelial cell line, PC12 cell line, rat pheochromocytoma cell line [30] and a graphene concentration range from 10 to 100 μg/mL or 200 μg/mL. Relatively weak toxicity was observed from graphene oxide and even at the highest concentration of 200 μg/mL, more than 80% cell viability was observed [29]. However, based on our study, graphene oxide has much lower cytocompatibility. The cell viability is estimated at 36.3% for PEG, 15.5% for DOC, and 6.3% for Pluronic P123 at a concentration of 100 μg/mL. These previous reports do not provide data on graphene functionalization, and according to our results, it is obvious that the dispersants significantly modify cytocompatibility of graphene oxide, most probably due to the direct toxicity and effects on graphene intracellular penetration. The results in the literature are inconsistent, particularly concerning the ability of graphene to enter the cells. For example, Wang et al. [31] demonstrated that graphene oxide aggregated in human fibroblast cells, but on the contrary, Chang et al. [29] reported that graphene oxide was hardly swallowed by A549 cells. The discrepancy may result from the different sample preparation and cell lines. The most probable mechanism underlying the toxicity of graphene oxide and reduced graphene oxide is oxidative stress, which is a well-accepted mechanism for nanoparticle toxicity and has in fact been and demonstrated on graphene [29,31–33].

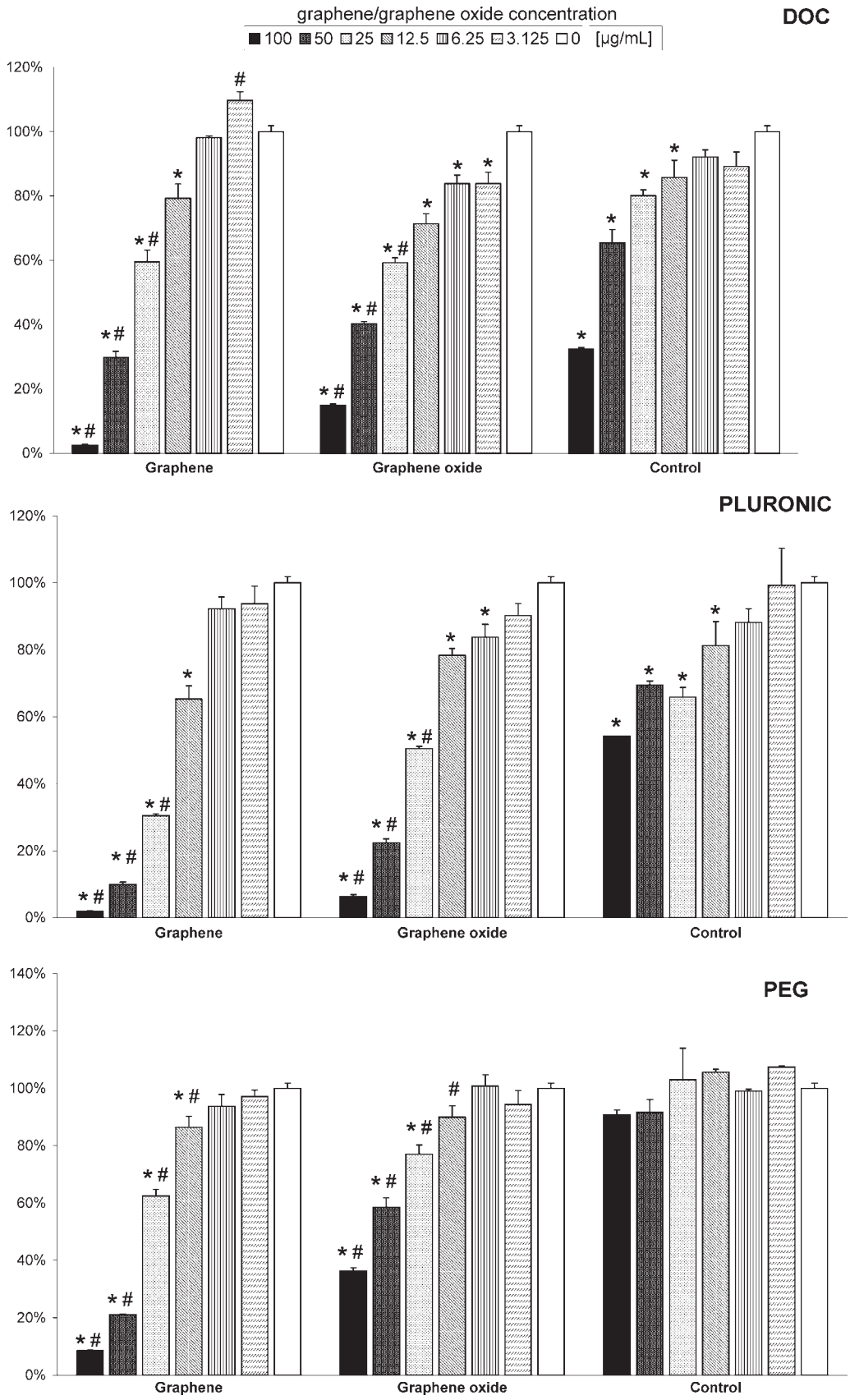

Fig. 8. Relative viability of L929 fibroblasts exposed to graphene oxide and reduced graphene oxide biofunctionalized with PEG, DOC or Pluronic P123. The cell viability is expressed as percentage of the value recorded for free growing cells. Control sets represent data for cells treated solely with respective dispersant at concentrations equal to those used for each graphene/graphene oxide concentration. Bars represent mean standard error of the mean (SEM). Significant differences (Student *t*-test) are marked with *(compared to free growing cells) or #(compared to corresponding concentration of the dispersant).

Previous data on carbon nanotubes (CNTs), which are most similar to graphene, show that its toxicity depends on the degree of functionalization [34]. For example, carboxylation of CNTs makes oxygen atoms abundant in oxygen atoms and decreases the toxicity. Graphene oxide contains many oxygen atoms in the carboxyl groups, epoxy groups, and hydroxyl groups [35] and so altered cytocompatibility is expected in case of reduced graphene oxide. Our results demonstrate that similar to graphene oxide, reduced graphene oxide in PEG is the most cytocompatible. Comparison between reduced graphene oxide and graphene oxide shows that the latter has better cytocompatibility, especially at higher concentrations like 50 and 100 μg/mL. The best biological properties are observed for graphene oxide functionalized with PEG whereas the other dispersants, Pluronic 123 and DOC, produce less favorable results.

5. Conclusion

We report the synthesis, dispersion, and toxicity of graphene oxide and reduced graphene oxide. The materials exhibit toxicity to mice fibroblast cells (line L929) and the degree depends on the concentration and type of dispersant. Both materials show relatively good cytocompatibility when the concentration is between 3.125 μg/mL and 12.5 μg/mL. Increasing the concentration of the nanomaterial in the dispersant reduces the cell viability and the lowest toxicity is detected from graphene oxide suspended in PEG.

Acknowledgements

The authors are grateful for the financial support of Foundation for Polish Science within FOCUS2010 Program, Hong Kong Research Grants Council (RGC) General Research Funds No. CityU 112510, City University of Hong Kong Applied Research Grant (ARG) No. 9667038.

References

[1] V.Y. Aristov, G. Urbanik, K. Kummer, D.V. Vyalikh, O.V. Molodtsova, A.B. Preobrajenski, et al., Nano Lett. 10 (2010) 992.
[2] H. Zhao, K. Min, N.R. Aluru, Nano Lett. 9 (2009) 3012.
[3] N.V. Medhekar, A. Ramasubramaniam, R.S. Ruoff, V.B. Shenoy, ACS Nano 4 (2010) 2300.
[4] S. Wang, M. Tambraparni, J. Qiu, J. Tipton, D. Dean, Macromolecules 42 (2009) 5251.
[5] Y. Chang, S.T. Yang, J.H. Liu, E. Dong, Y. Wang, A. Cao, et al., Toxicol. Lett. 200 (2010) 201.
[6] K. Kostarelos, A. Bianco, M. Prato, Nat. Nanotechnol. 4 (2009) 627.
[7] Z. Liu, S. Tabakman, K. Welsher, H. Dai, Nano Res. 2 (2009) 85.
[8] Y.X. Huang, P.V. Palkar, L.J. Li, H. Zhang, P. Chen, Biosens. Bioelectron. 25 (2010) 1834.
[9] K. Yang, J. Wan, S. Zhang, Y. Zhang, S.T. Lee, Z. Liu, ACS Nano 5 (2010) 516.
[10] X. Sun, Z. Liu, K. Welsher, J.T. Robinson, A. Goodwin, S. Zaric, H. Dai, Nano Res. 1 (2008) 203.
[11] Z. Liu, J.T. Robinson, X.M. Sun, H.J. Dai, J. Am. Chem. Soc. 130 (2008) 10876.
[12] K. Wang, J. Ruan, H. Song, J. Zhang, Y. Wo, S. Guo, et al., Nanoscale Res. Lett. 10 (2010) 1303.
[13] D.C. Marcano, D.V. Kosynkin, J.M. Berlin, A. Sinitskii, Z. Sun, A. Slesarev, et al., ACS Nano 4 (2010) 4806.
[14] C. Zhu, S. Guo, Y. Fang, S. Dong, ACS Nano 4 (2010) 2429.
[15] G. Wang, B. Wang, J. Park, J. Yang, X. Shen, J. Yao, Carbon 47 (2009) 68.
[16] G. Lazar, K. Zellamaa, I. Vascan, M. Stamate, I. Lazar, I. Rusu, J. Optoelectr. Adv. Mater. 7 (2005) 647.
[17] S. Wang, S.P. Jiang, X. Wang, Electrochem. Acta 56 (2011) 3338.
[18] Z.J. Fan, W. Kai, J. Yan, T. Wei, L.J. Zhi, J. Feng, et al., ACS Nano 5 (2011) 191.
[19] H.K. Jeong, Y.P. Lee, R.J.W.E. Lahaye, M.H. Park, K.H. An, I.J. Kim, et al., J. Am. Chem. Soc. 130 (2008) 1362.
[20] N.R. Wilson, P.A. Pandey, R. Beanland, R.J. Young, I.A. Kinloch, L. Gong, et al., ACS Nano 3 (2009) 2547.
[21] Z. Ni, Y. Wang, T. Yu, Z. Shen, Nano Res. 1 (2008) 273.
[22] A.C. Ferrari, Solid State Commun. 143 (2007) 47.
[23] A.C. Ferrari, J. Robertson Phys. Rev. B 61 (2000) 14095.
[24] K.N. Kudin, B. Ozbas, H.C. Schniepp, R.K. Prud'homme, I.A. Aksay, R. Car, Nano Lett. 8 (2007) 36.
[25] A.C. Ferrari, J.C. Meyer, V. Scardaci, C. Casiraghi, M. Lazzeri, F. Mauri, et al., PRL 97 (2006) 187401.
[26] S. Zhang, P. Xiong, X. Yang, X. Wang, Nanoscale 3 (2011) 2169.
[27] Biological evaluation of medical devices. Part 5: Tests for in vitro cytotoxicity. ISO 10993-5, 2009.
[28] L. Feng, S. Zhang, Z. Liu, Nanoscale 3 (2011) 1252.
[29] Y. Chang, S.T. Yang, J.H. Liu, E. Dong, Y. Wang, A. Cao, et al., Toxicol. Lett. 200 (2011) 201.
[30] Y. Zhang, S.F. Ali, E. Dervishi, Y. Xu, Z. Li, D. Casciano, et al., ACS Nano 4 (2010) 3181.
[31] K. Wang, J. Ruan, H. Song, J. Zhang, Y. Wo, S. Guo, et al., Nanoscale Res. Lett. 5 (2010) 1.
[32] N. Lewinski, V. Colvin, R. Drezek, Small 4 (2008) 26.
[33] N. Li, T. Xia, A.E. Nel, Free Radic. Biol. Med. 44 (2008) 1689.
[34] C.M. Sayes, F. Liang, J.L. Hudson, J. Mendez, W. Guo, J.M. Beach, et al., Toxicol. Lett. 161 (2006) 135.
[35] D.R. Dreyer, S. Park, C.W. Bielawski, R.S. Ruoff, Chem. Soc. Rev. 39 (2010) 228.